

# Additive Layer by Layer Simulation and Taguchi Loss of Function for AlSi10Mg Alloy Samples Manufactured by Selective Laser Melting

Mudda Nirish<sup>1</sup> and R Rajendra<sup>2</sup>

<sup>1</sup>Research Scholar of Mechanical Engineering Department, University College of Engineering (A), Osmania University, Telangana, India.

<sup>2</sup>Professor of Mechanical Engineering Department, University College of Engineering (A), Osmania University, Telangana, India.

## ABSTRACT:

The significance of the selective laser melting (SLM) component depends on build orientation and layer thickness, which are directly influenced by processing parameters. This paper presents research done by layer by layer AM simulation before the printing process, such as saving of time, cost, and material used with different process parameters such as laser power, scan speed, and hatching distance. The considered process parameters are based on the AM simulation (i.e., less displacement at low temperature than is produced in the SLM printing process). According to the design of the experiment, the samples were printed as per ASTM standard samples to find out the Taguchi loss of function for after manufactured SLM parts, such as part geometric inaccuracy observed by the Artec 3D scanner. All the process parameters were obtained without loss of function at 225 watts, 500 mm/s, and 100  $\mu$ m as T5.

**Keywords:** Additive Manufacturing (AM), Laser Powder Bed Fusion (LPBF), Selective Laser Melting (SLM), AlSi10Mg Alloy, Geometric Dimensioning and Tolerance (GD&T), Taguchi Loss of Function.

## 1. INTRODUCTION

### 1.1 Background

The selective laser melting (SLM), also called direct metal laser melting (DMLM), is a layer-by-layer manufacturing technology with fully dense and high-quality metal parts produced by the corresponding 3D-Computer Aided Design (CAD) model [1,2]. The biggest drawback that limits the applicability of today's technologies is the high cost of AM components [3]. Metal AM provides the advantages of being flexible in terms of geometric design and wasting less material in the AM process [4,5]. The current trend to increase productivity or efficiency is based on the process parameters of optimization technology [6], multi laser machine process development [7], and automation aimed at reducing machine downtime while producing high-density parts [8]. The low intensity of these profiles can reduce evaporation and increase the maximum energy input [9,10]. AM technology has built up within the defense, aerospace, and biomedical industries [11]. In SLM fabricated samples, three types of porosity are present: "lack of fusion", gas and shrinkage porosity, and key holing [12]. "Lack of fusion" is a bonding defect that arises in parts with a low energy density or low laser power [13,14].

Previous researchers have worked on the microstructure and mechanical properties of parts made of AlSi10Mg: powder properties [15], internal porosity of defective parts [16], hardness, surface roughness, and tensile properties [17]. The very few people were done after manufacturing parts to find geometric dimensioning and tolerance (GD&T) and Taguchi loss of function [18,19]. The main effects in the AM printing process concluded that build orientation was the best process parameter and that there could be the most influence on density [20,21]. The optimized parameters are empirically derived to generally produce dense materials, minimize defects [22], reduce surface roughness [23], increase build rate, and produce parts with acceptable material properties [24,25].

### 1.2. Scope of the present work

In this work studied Taguchi loss of function after SLM parts are manufactured based on the given process parameter as L9 OA.

- From the literature survey identified the SLM printing process parameters.
- Developed the AM simulation according to L9 OA.
- Using the Artec 3D scanner for geometric dimensioning and tolerance and calculate the loss of function for geometric inaccuracy.

## 2. EXPERIMENTAL PROCEDURE

### 2.1 Material

The laser melted AlSi10Mg alloy parts are fabricated by the SLM process. The chemical formula for AlSi10Mg is shown in table 1. The power particle size distribution has the main importance in the SLM process because it has the main influence on the part qualification, i.e., performance. The powder particle size distribution ranged from 20 to 63  $\mu\text{m}$  and it was supplied by SLM solution group AG, Germany. The powder weighted residual is 0.694%, the specific surface area is 0.154  $\text{m}^2/\text{g}$ , the surface weighted mean is 38.8  $\mu\text{m}$  and the volume weighted mean is 43.5  $\mu\text{m}$ . The sample was prepared for SLM printing as per the ASTM standard E2948 and the specimen dimensions were 130×11 mm total length and 45×7.5 mm gauge with a radius of 7.5 mm.

Table 1: Chemical composition of AlSi10Mg alloy.

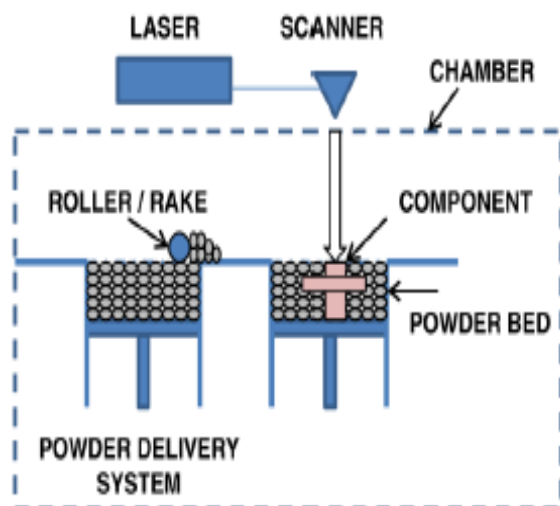
Al	Si	Fe	Cu	Mn	Mg	Zn	Ti	Ni	Pb	Sn	Other total
Balance	9.00 – 11.00	0.55	0.05	0.45	0.20 – 0.45	0.10	0.15	0.05	0.05	0.05	0.15

### 2.4 SLM process

The SLM process parameters for Taguchi loss of function use the laser power (P), layer thickness (t), beam diameter (D), material feed ( $m_p$ ), hatching distance (h), scan speed (v), and building directions (BD or d) (X, Y, and Z axis). These are the adjustable parameters for layer thickness, laser power, scanning speed, hatch spacing, and recoater speed (machine/material dependent). All the specimens were fabricated according to the Taguchi L9 orthogonal array (OA) by producing an SLM machine M280 model of AlSi10Mg alloy as shown in figure 2. The powder particle distribution used in our experiments ranged from 20 to 63  $\mu\text{m}$ . The powder feed rate during the printing process was 2 to 5  $\mu\text{m}$  and the applied cooling rate was 120 to 320 seconds for each layer. The SLM build platform dimensions are 280 × 280 × 365 mm and use a continuous IPG fiber laser. As shown in table 2, the process parameters that varied in this study were laser power at three levels of 200, 225, and 250 Watts; scan speed at three levels of 400, 500, and 600 mm/s; and hatch distance at three levels of 60, 80, and 100  $\mu\text{m}$ . The remaining process parameters are kept constant; the laser spot diameter is 75  $\mu\text{m}$ , layer thickness is 30  $\mu\text{m}$ , build platform temperature is 150°C and scanning pattern is 0°. All the specimens were built in a horizontal orientation (i.e. without any support structure) as shown in figure 1 and used only printing support on the SLM-base plate (i.e. block support structure). In the printing process, maintain the air atmosphere at a maximum oxygen content level of 0.12%.

Table 2: used L9 orthogonal array as per DoE.

Parameters	Level 1	Level 2	Level 3
A: Laser power (LP) in Watts	200	225	250
B: Scan speed (SS) in mm/s	400	500	600
C: Hatching distance (HD) in $\mu\text{m}$	60	80	100



(a)

(b)

Figure 1: SLM schematic diagram and printing process.

### 3. RESULTS AND DISCUSSION

#### 3.1 Simulation of part using experimental design table

The temperature variation is the main important process in the SLM printing process and is also done for AM simulation for thermal analysis (i.e., saving cost, time, and material). The optimized process parameter used as L9 OA before SLM printing is shown in figure 2. The AM simulation results are represented in figure 3 and also in table 3. From the simulation results, trail 5 produced better results with less temperature and less displacement while in the SLM printing process. This process parameter was considered to avoid defects and thermal deviation with high strength. If the part was printed at a high temperature, it required a high cooling rate and produced defects with thermal defects (i.e., inaccurate geometry).

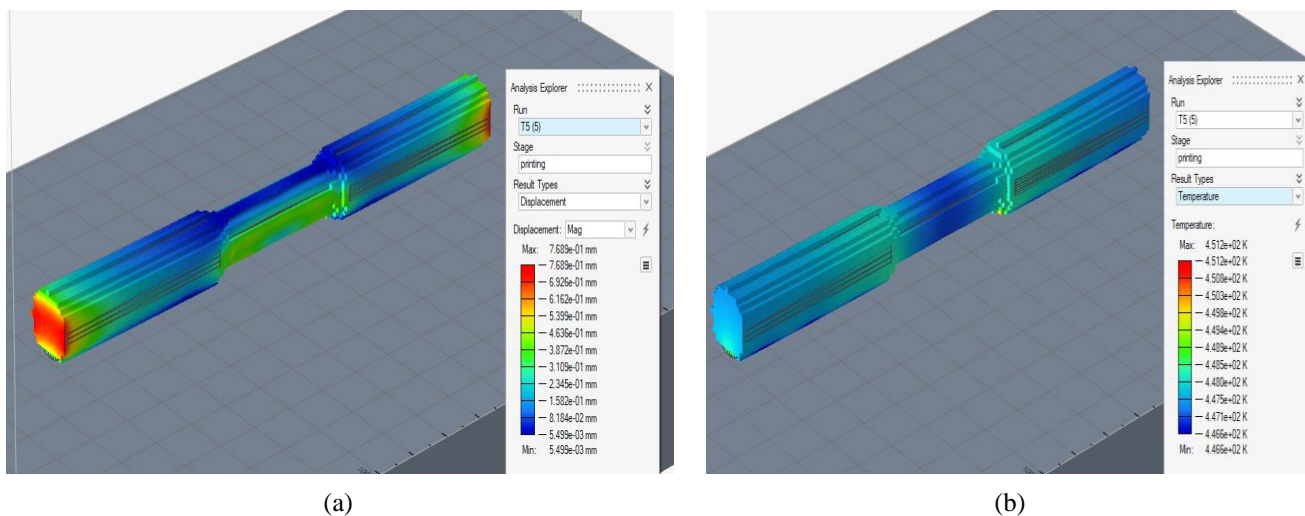


Figure 2. Thermal simulations of displacement and SLM printing temperatures used in printing process

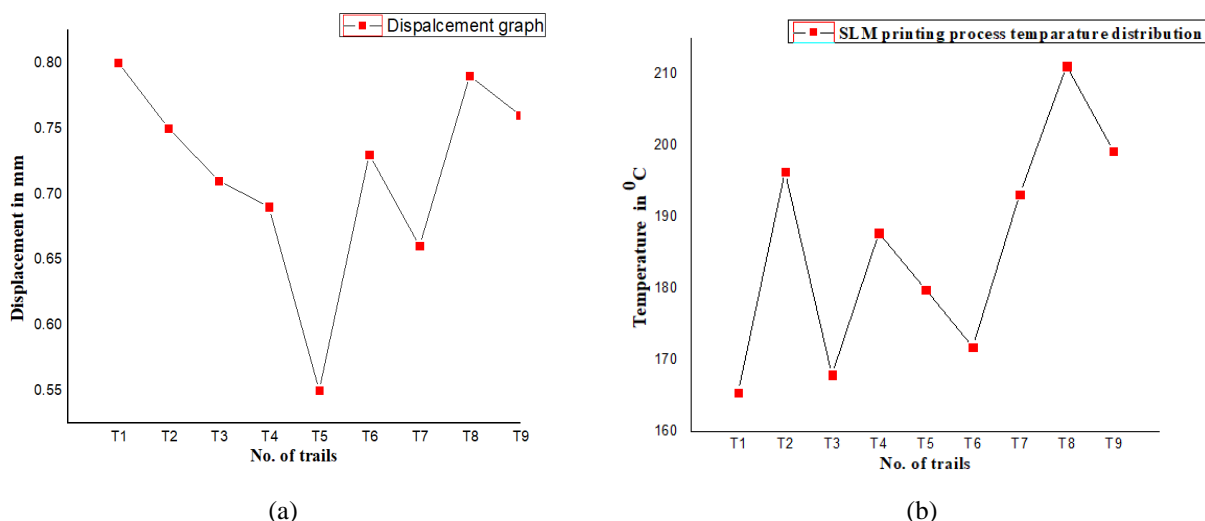


Figure 3: Thermal analysis of displacement and SLM printing process temperature.

Table 4: Thermal simulation results.

Trails	Displacement in mm	Plastic strain	Von mises stress in MPa	Temperature in °C
T1	0.80	0.37	97.16	165.35
T2	0.75	0.32	95.66	196.25
T3	0.71	0.31	115.3	167.85
T4	0.69	0.43	107.1	187.65
T5	0.55	0.38	236.6	179.75
T6	0.73	0.33	109.3	171.75
T7	0.66	0.45	105.6	193.05
T8	0.79	0.37	96.41	210.95
T9	0.76	0.33	95.08	199.05

### 3.2 Geometric accuracy of part

The measured geometric dimensions for part geometry accuracy were used on an Artec 3D scanner with a high-resolution white laser. The technology used in this research scanned the after SLM manufactured parts and observed the current geometric shape (such as thermal distortion and deviation) based on the given L9 OA process parameter. Then, as shown in figure 4, they compare the nominal diameter (i.e., design diameter) with the SLM printed diameter and calculate the Taguchi loss of function at each part. The given design diameters as gauge is 7.5 mm in diameter with a 40 mm length at the top and bottom, and 11 mm in diameter with a 45 mm length. The specimen dimensions (bottom, top, and gauge) were increased due to the high laser with low scan rate as shown in figure 5.

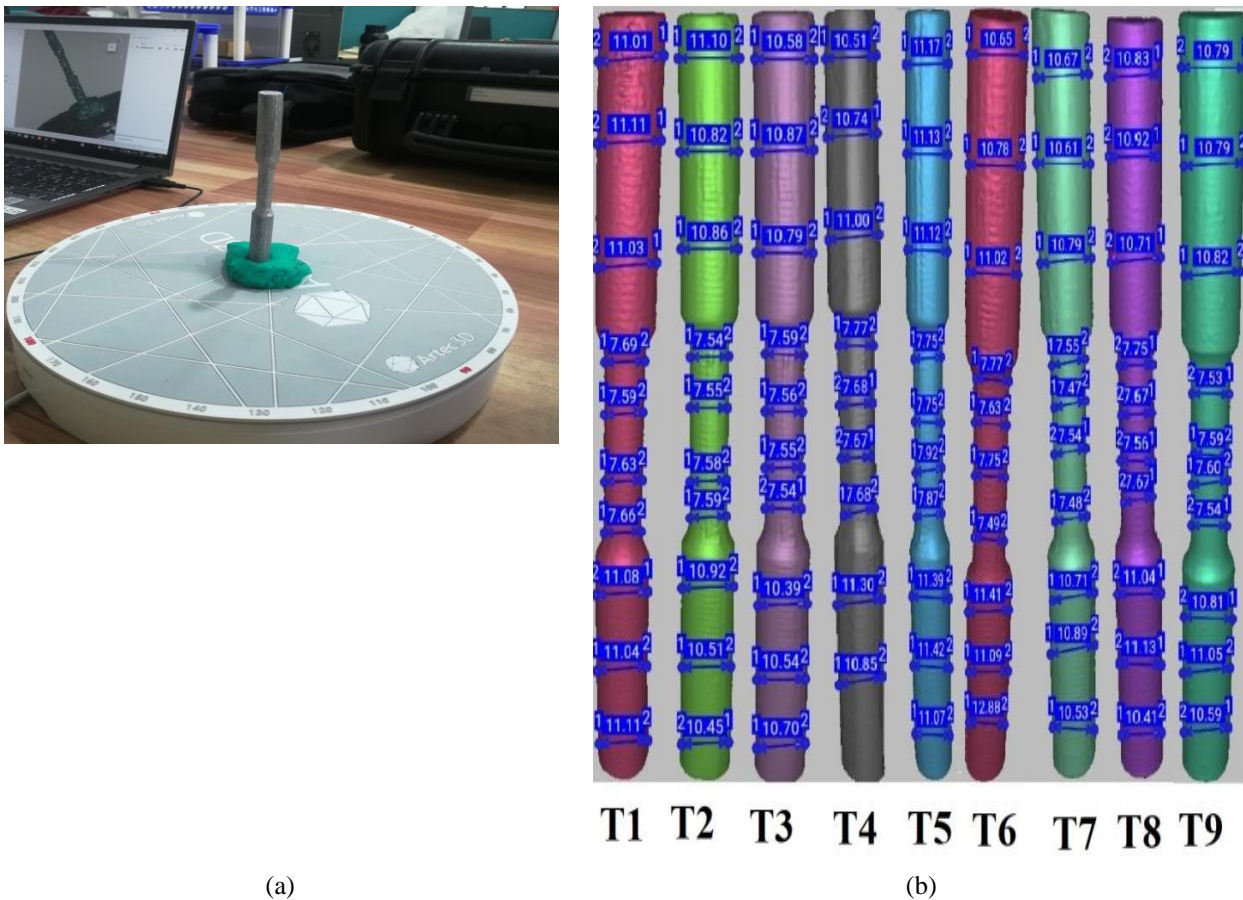


Figure 4: Artec 3D scanning for part geometry and part printed is located and scanned diametrical deviation of top, middle and lower diameter section (T5 part give dimensionally accurate geometry).

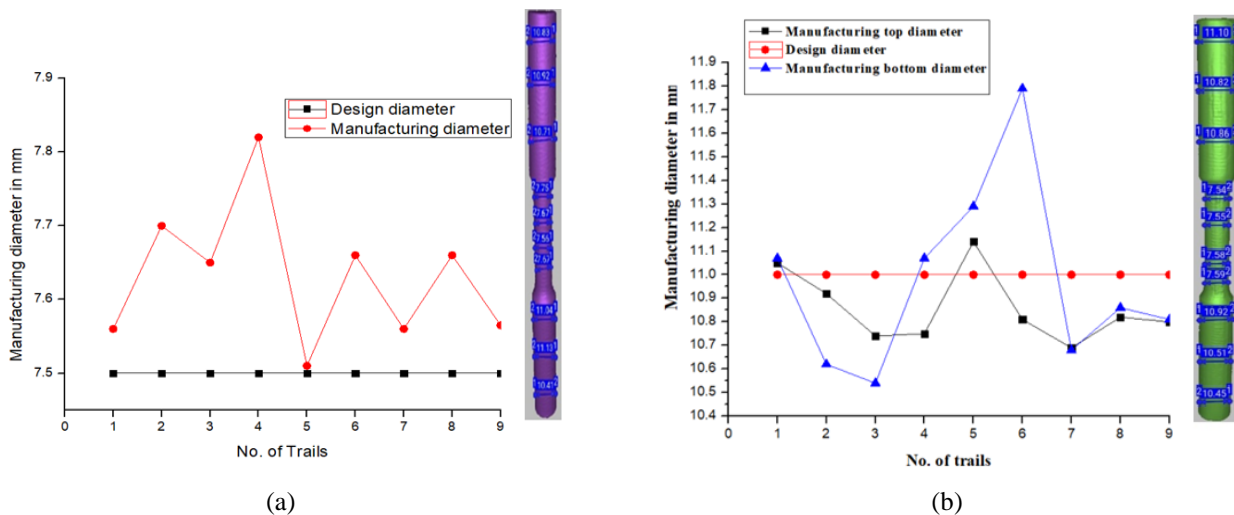


Figure 5: (a & b) Compared the diameters with design diameter.

### 3.3 Taguchi loss of functions for geometric inaccuracy

The product is shipped to the customer after being manufactured, and all parts have a constant cost of 36,000 Rs. The results were obtained after printing all specimens with the upper limit (UL) and comparing them to design diameter values. As shown in figure 5, the maximum loss of function dimensions is between 7.51 and 7.82 mm. The Taguchi loss of function is calculated by the

equation of  $L = k (y-m)^2$ ... (eq.1), where L is the loss of function of each part, k is the constant cost of all the specimens (i.e. each specimen cost was 4000 Rs/-), y is the specimen gauge diameter (i.e. the design diameter is 7.5 mm) and m is the manufactured diameter in mm. The loss of function results in each part, as shown in table 5.

Table 5: Geometric dimensional due to part inaccuracy.

Trails	Specimen gauge diameters in mm	Deviation of specimen diameter in mm (y-m)	(y-m) <sup>2</sup>	Loss of function (L = K (y-m) <sup>2</sup> ) as each part in Rs/-
T1	7.56	0.06	0.0036	14.4
T2	7.7	0.2	0.04	160
T3	7.65	0.15	0.0225	90
T4	7.82	0.32	0.1024	409.6
T5	7.50	0.0	0.0	0.0
T6	7.66	0.16	0.0256	102.4
T7	7.56	0.06	0.0036	14.4
T8	7.66	0.16	0.0256	102.4
T9	7.57	0.07	0.0049	19.6
Total no. of parts = 9				Totals loss = 913.2 /-

#### 4. CONCLUSION

In this research, SLM parts were printed after AM layer simulation based on the L9 OA with horizontal building orientations, and the geometric inaccuracy dimensions were measured using an Artec 3D scanner to find the Taguchi loss of function.

- It is observed that when using a high laser at the different scan speeds in the AM simulation process, the simulation results are given the part displacement (i.e., deviation) due to high laser power operated in the SLM process. Consider values like low laser power with a lower scan speed rate for high density and mechanical strength.
- A very high SS of 600 mm/s was given a high percentage of porosity, pores, and cracks, i.e., resulting in a drastic reduction in mechanical properties like strength and hardness.
- Finally, achieved a (T5) defect-free component without distortion at these process parameters, such as laser power is 225 Watts, scan speed is 500 mm/s, and hatching distance is 100 µm, energy density is 150 J/mm<sup>3</sup>.

#### References

1. Shahrubudin N, Lee TC, Ramlan R. An overview on 3D printing technology: Technological, materials, and applications. *Procedia Manufacturing*. 2019, 1; 35, 1286-96.
2. Mançanares CG, Zancul ED, da Silva JC, Miguel PA. Additive manufacturing process selection based on parts' selection criteria. *The International Journal of Advanced Manufacturing Technology*. 2015, 80(5), 1007-14.
3. Wang Y, Blache R, Xu X. Selection of additive manufacturing processes. *Rapid prototyping journal*. 2017.
4. Nirish M, Rajendra R. Suitability of metal additive manufacturing processes for part topology optimization–A comparative study. *Materials Today: Proceedings*. 2020, 27, 1601-7.
5. Wang P, Lei H, Zhu X, Chen H, Fang D. Influence of manufacturing geometric defects on the mechanical properties of AlSi10Mg alloy fabricated by selective laser melting. *Journal of Alloys and Compounds*. 2019, 789, 852-9.
6. Li R, Chen H, Zhu H, Wang M, Chen C, Yuan T. Effect of aging treatment on the microstructure and mechanical properties of Al-3.02 Mg-0.2 Sc-0.1 Zr alloy printed by selective laser melting. *Materials & Design*. 2019, 168, 107668.
7. Rometsch P, Jia Q, Yang KV, Wu X. Aluminum alloys for selective laser melting–towards improved performance. *In Additive Manufacturing for the Aerospace Industry*. Elsevier. 2019, 301-325.
8. Ferro P, Meneghello R, Razavi SM, Berto F, Savio G. Porosity inducing process parameters in selective laser melted AlSi10Mg aluminium alloy. *Physical Mesomechanics*. 2020, 23(3), 256-62.
9. Liu Y, Liu C, Liu W, Ma Y, Tang S, Liang C, Cai Q, Zhang C. Optimization of parameters in laser powder deposition AlSi10Mg alloy using Taguchi method. *Optics & Laser Technology*. 2019, 111, 470-80.
10. Read N, Wang W, Essa K, Attallah MM. Selective laser melting of AlSi10Mg alloy: Process optimisation and mechanical properties development. *Materials & Design*. 2015, 65, 417-24.

11. Wu H, Li J, Wei Z, Wei P. Effect of processing parameters on forming defects during selective laser melting of AlSi10Mg powder. *Rapid Prototyping Journal*. 2020.
12. Samantaray M, Thatoi DN, Sahoo S. Modeling and optimization of process parameters for laser powder bed fusion of AlSi10Mg alloy. *Lasers in Manufacturing and Materials Processing*. 2019, 6(4), 356-73.
13. Nirish M, Rajendra R. Heat Treatment Effect on the Mechanical Properties of AlSi10Mg Produced by Selective Laser Melting. *Journal of mechanical engineering research and development*. 9:11-00.
14. Kempen K, Thijs L, Van Humbeeck J, Kruth JP. Mechanical properties of AlSi10Mg produced by selective laser melting. *Physics Procedia*. 2012, 39, 439-46.
15. Li Y, Gu D. Parametric analysis of thermal behavior during selective laser melting additive manufacturing of aluminum alloy powder. *Materials & design*. 2014, 63, 856-67.
16. Gao C, Wu W, Shi J, Xiao Z, Akbarzadeh AH. Simultaneous enhancement of strength, ductility, and hardness of TiN/AlSi10Mg nanocomposites via selective laser melting. *Additive Manufacturing*. 2020, 34, 101378.
17. Pei W, Zhengying W, Zhen C, Junfeng L, Shuzhe Z, Jun D. Numerical simulation and parametric analysis of selective laser melting process of AlSi10Mg powder. *Applied Physics A*. 2017, 123(8), 1-5.
18. Tradowsky U, White J, Ward RM, Read N, Reimers W, Attallah MM. Selective laser melting of AlSi10Mg: Influence of post-processing on the microstructural and tensile properties development. *Materials & Design*. 2016, 105, 212-22.
19. Nirish M & Rajendra R. Additive Simulation and Process Parameter Optimization for Wear Characterization Development by Selective Laser Melting of AlSi10Mg Alloy. *Journal of Characterization*. Vol.2 (2). ISSN: 2757-9166. Pp.103-116.
20. Trevisan F, Calignano F, Lorusso M, Pakkanen J, Aversa A, Ambrosio EP, Lombardi M, Fino P, Manfredi D. On the selective laser melting (SLM) of the AlSi10Mg alloy: process, microstructure, and mechanical properties. *Materials*. 2017, 10(1), 76.
21. Uzan NE, Shneck R, Yeheskel O, Frage N. Fatigue of AlSi10Mg specimens fabricated by additive manufacturing selective laser melting (AM-SLM). *Materials Science and Engineering: A*. 2017, 704, 229-37.
22. Nirish M, Rajendra R. Effect of Heat Treatment on Wear Characterization of AlSi10Mg Alloy Manufactured by Selective Laser Melting ; 9:11-00.
23. Bai P, Huo P, Kang T, Zhao Z, Du W, Liang M, Li Y, Liao H, Liu Y. Failure Analysis of the Tree Column Structures Type AlSi10Mg Alloy Branches Manufactured by Selective Laser Melting. *Materials*. 2020, 13(18), 3969.
24. Santos LM, Ferreira JA, Jesus JS, Costa JM, Capela C. Fatigue behaviour of selective laser melting steel components. *Theoretical and Applied Fracture Mechanics*. 2016, 85, 9-15.
25. Nirish M & Rajendra R. Optimization of Process Parameter and Additive Simulation for Fatigue Strength Development by Selective Laser Melting of AlSi10Mg Alloy. *International Journal of Mechanical Engineering*. Vol.7 (2). ISSN: 0974-5823. pp.3795-3802.2022.